Petroleum and Coal

Article **Open Access**

Airborne and Satellite Geophysical Data Interpretation of the Gubio Area in the Bornu Basin, Northeastern Nigeria: Implication for Hydrocarbon Prospectivity

Daniel N. Obiora[1], Bernadette C. Dimgba[1], Ifeanyi. A. Oha[2], Johnson C. Ibuot[1]*

[1] Department of Physics and Astronomy, University of Nigeria, Nsukka, Enugu State, Nigeria
[2] Department of Geology, University of Nigeria, Nsukka, Enugu State, Nigeria

Received July 16, 2019; Accepted November 2, 2020

Abstract

The Gubio area came into international limelight on the 25th of July 2017 when four oil exploration personnel were abducted while collecting data around Gubio. This resulted in the unfavourable halt of exploration in the region amidst fears of rising insecurity. This contribution is aimed at analyzing airborne and satellite geophysical data of the area to determine the sediment thickness and thus comment on the hydrocarbon prospectivity in the area. Standard Euler deconvolution and Source Parameter Imaging (SPI), in addition to inverse modelling methods, were employed. The SPI estimated depth from aeromagnetic interpretation ranges from 381.7 m to 4610.5 m. The depth estimated from Euler depth analysis for the structural index of SI = 0 ranges from 1260.5 to 3968.5 m. The estimated depth from forward and inverse modeling for profiles 1-6 were 709, 722, 2052, 1836, 4365 and 877 m, with respective susceptibility values of 0.0003, 0.017, 0.04, 0.025, 0.0002 and – 0.0001. From satellite gravity data interpretation, estimated SPI depth ranges from 1009.3 to 4511.9 m; Euler depth estimation to anomalous bodies ranges from 1696.8 to 4371.2 m; while modelling depth estimation for profiles 7 and 8 were 3460 m and 1250 m with respective density values of 2.700 and 2.630 g/cm^3. These depth ranges and distribution of anomalies in the area favours a promising basin in terms of hydrocarbon prospectivity.

***Keywords**: Aeromagnetic and satellite gravity data; Gubio, Bornu Basin; Source parameter imaging; Euler deconvolution; modelling.*

1. Introduction

The Gubio area falls within the Chad Basin, which has been described as the largest inland basin in Africa with an area in excess of 2,300,000 km^2 [1]. The importance of this large inland basin in terms of hydrocarbon potential has grown significantly especially after the discovery of the first oil deposit in the region by Conoco in 1974, after which over 13 oil discoveries and three gas discoveries were made. The Nigerian part of the basin is called the Bornu Basin, which makes up only 10% of the entire basin [2]. The search for hydrocarbon in the Bornu Basin intensified after the Conoco find of 1974, and about 23 wells have been drilled so far with no economic find. Three dry wells, namely, Gubio-1, Ngor-1, and Ngamma-1 were drilled around the Gubio area by the Nigerian National Petroleum Company (NNPC). In the past five years, the NNPC has indicated more strongly its resolve to explore the basin by embarking on detailed ground magnetic and gravity surveys in addition to detailed sampling of shales for organic geochemical analysis. This quest suffered a huge setback on the 25th of July 2017 when oil exploration workers affiliated with NNPC and the Department of Geology, University of Maiduguri were abducted by members of "Boko Haram" between Gubio and Magumeri, about 80km north of Maiduguri town. The glaring poor security situation in the region may constitute an enormous hindrance to the regional exploration progress, hence the need to take a critical look at existing airborne and satellite geophysical data and to attempt a re-appraisal of the basin configuration around the Gubio area through inverse modelling.

Airborne and satellite geophysics forms a critical component of geological mapping and mineral resource inventory programmes in many countries. The Nigerian Geological Survey Agency (NGSA) engaged Fugro Airborne Surveys to carry out a nationwide aeromagnetic and airborne radiometric survey in 2005. The Survey began in May 2005 and was completed in September 2007. These data have over the years provided an alternative source of information and contributing significantly to what is known in the geology of many parts of Nigeria. They also contribute to petroleum and mineral exploration, mining and environmental protection application [3]. Satellite gravity is acquired using the Grace Gravity Model Sensor, which is mounted on-board two satellites and the bouguer gravity anomaly is measured at the sensor.

The Bornu Basin has been studied in terms of stratigraphy [2,4-6], hydrocarbon potential [1-2,7-9], and geophysical signatures [7-8,10-13]. This study employed a novel approach of integrating satellite gravity and aeromagnetic data for the Gubio area. The goal is to ascertain how each method can complement the other for better subsurface mapping of structures in parts of the Bornu Basin. Earlier geophysical works carried out in the Bornu Basin employed either ground gravity data or airborne magnetic data; a combination of these two data analyses will yield better results, as the limitation of one will be compensated by the other.

2. Location and geology of the study area

The study area forms part of the West and Central African Rift System (WCARS) (Fig. 1) whose origin is attributed to the separation between Africa and South America as a result of the breakup of the Gondwana [14-16].

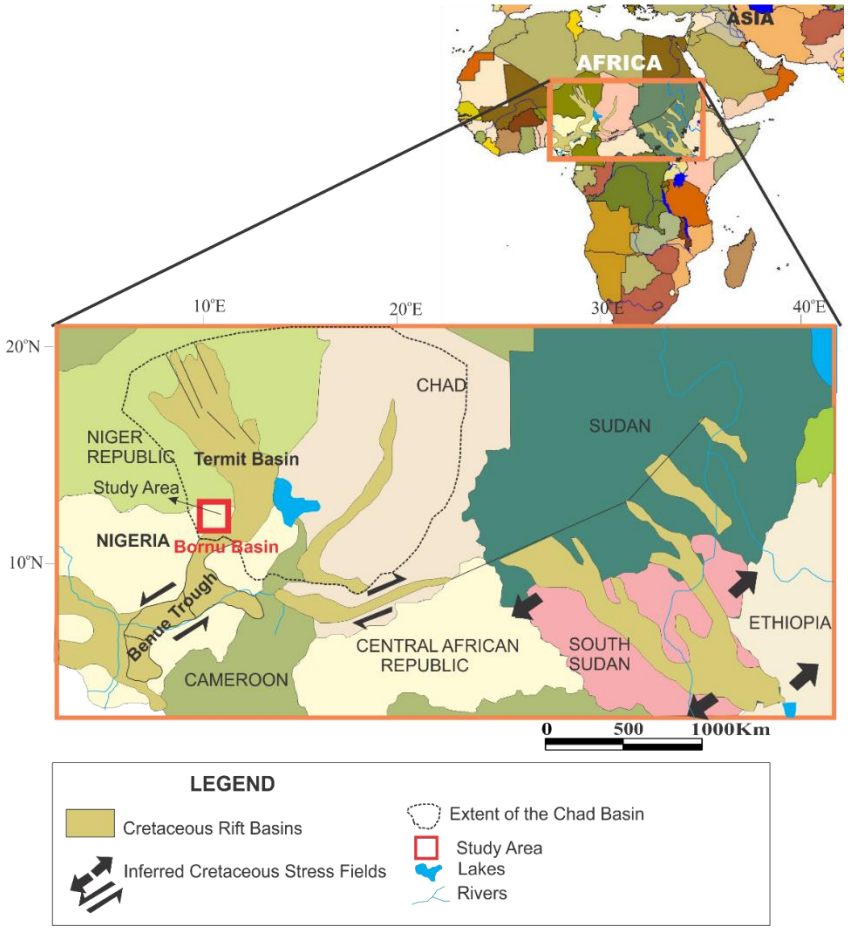

Fig. 1 Map of West and Central African Rift systems showing the extent of the Chad Basin, location of Bornu Basin and position of the study area (modified after [19])

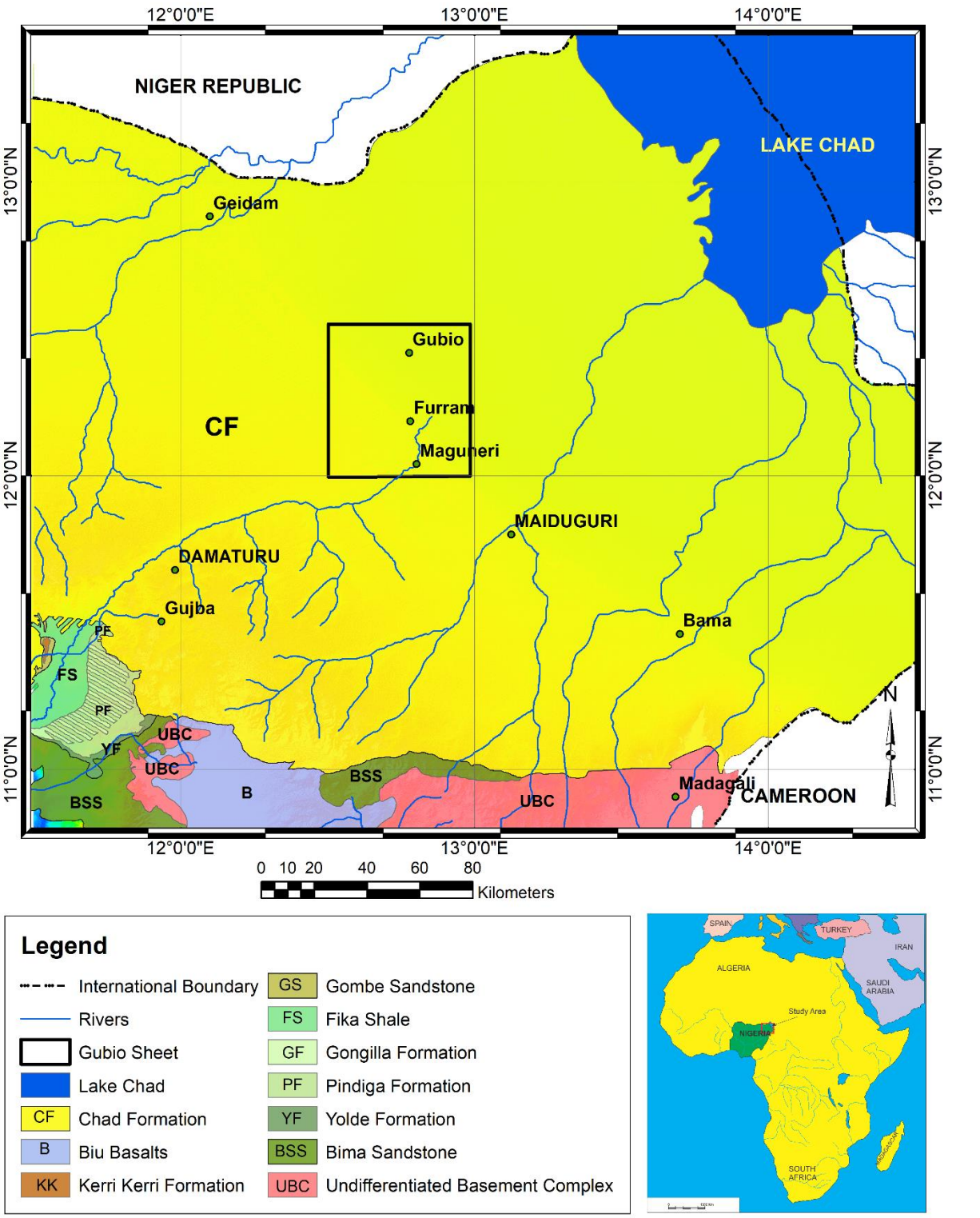

Fig. 2 Geological map of the Bornu Basin, showing the location of Gubio area. Inset is the map of Africa showing the location of Nigeria and the study area

The area lies within latitudes 12.0° to 12.5°N and longitude 12.5° to 13.0°E covering an area of approximately 3025km^2 (see Fig. 3). Chad Basin has been described as a broad sediment-filled depression stranding northeastern Nigeria and adjourning parts of the Chad and

Niger Republic [1]. However, recent ideas have postulated the subsurface of the area as belonging to the northern part of the Benue Trough [17]. Its origin has been generally attributed to the rift system that developed in the early Cretaceous when the African and South American Lithospheric plates separated, and the Atlantic opened [16]. The oldest sediment in the area consists of shallow marine sediments referred to as pre-Bima, which unconformably overlies the Basement Complex rocks. This is overlain by the thick sequence of the continental Bima Sandstone which represents a major regressive event prevalent during Albian – Cenomanian times. The Bima Sandstone is overlain conformably by the transitional Gongila Formation, which consists of basal limestone and sandstone/shale sequence. The blue-black Fika Shales overlie the Gongila Formation conformably and appear to have been deposited under a submerged (transgression) environment (Fig. 3). These Shales are occasionally gypsiferous and contain thin persistent limestone. The Gombe Sandstone is a continental sequence of estuarine and deltaic sediments deposited over the marine Fika Shales. This Formation consists of lenses of siltstones and mudstone with ironstone at the lower beds. The middle part is characterized by well-bedded sandstone and siltstone [18], while the upper part contains poor quality coals and characterized by cross-bedded sandstone.

The end of the Cretaceous was marked by a period of widespread uplift and erosion. The first deposits in the Nigerian sector of the basin after this period is the loosely cemented coarse to fine-grained sandstone – the Kerri-Kerri Formation. Massive claystone and siltstone with bands of ironstone and conglomerate occur locally in this Formation. The sandstones are often cross-bedded, and lignite (low-grade coal) occurs near the base of the Formation. Angular unconformity was thought to exist between the Kerri-Kerri Formation and the Gombe Sandstone. The Chad Formation is Pleistocene in age and composed of an argillaceous sequence in which three well defined arenaceous horizons occur. A minor unconformity indicated by a plinth of laterite is identified in a borehole as separating the Kerri -Kerri Formation from the Chad Formation [12]. Figure 2 shows the geological map of the Bornu basin and marks the position of the Gubio area.

PERIOD/ EPOCH/AGE	FORMATION	LITHOLOGY	AVERAGE THICKNESS (m)	THICKNESS FROM SEISMIC DATA (m)	OUTCROP DESCRIPTION	SUBSURFACE INTERPRETATION FROM SEISMIC DATA (m)
QUATERNARY	CHAD		400	800 (Average)	Variegated clays with Sand Interbeds.	
TERTIARY	KERRI-KERRI		130		Iron-rich Sandstones and clay covered by laterite plinths.	
MAASTRICHTIAN	GOMBE		315	0 - 1,000	Sandstone + Siltstone + Clay with Coal seams. Fossils: Bivalve impressions and Cruziana labens purren.	
SENONIAN	FIKA		430	0 - 900	Dark grey to black gypsiferous shale with limestone interbeds	
TURONIAN	GONGILA		420	0 - 800	Alternating sequence of sandstone and shale with limestone interbeds	
CENOMANIAN	BIMA		3,050	2,000	Poorly sorted gravely to medium-grained highly feldspathic sandstone.	
ALBIAN	?? UNNAMED			3,600		Seismically transparent sequence (A monolithological sequence is inferred)
	?? UNNAMED			0 - 3,000		Piedmont Alluvial fans and early rift sediments
PRECAMBRIAN	BASEMENT COMPLEX					

LITHOLOGY LEGEND: Sandstone Shale Igneous & Metamorphic Rocks

Fig. 3. Generalized Stratigraphic Sequence of Chad Basin, Nigeria (after [7])

3. Source of data

The high resolution airborne magnetic data of Gubio (sheet 66) used for this study, was obtained from the Nigerian Geological Survey Agency (NGSA). The satellite gravity data were obtained in 2013 using GRACE GRAVITY MODEL Sensor on-board two satellites by National Aeronautics and Space Administration (NASA) and German Aerospace Center. The aeromagnetic data were acquired using a 3 x Scintrex CS2 caesium vapour magnetometer by Fugro Airborne Surveys between 2007 and 2009. The airborne magnetic survey was flown at a terrain clearance of 80 m along flight lines spaced 500 m apart. The flight line direction was 135°, with tie lines perpendicular (225°). The Gubio aeromagnetic data were recorded in digital form (X, Y, Z text file) after removing the geomagnetic reference field (IGRF). The X and Y represent the longitude and latitude of Gubio in meters, while the Z represents the magnetic field intensity measured in nanoTesla. The airborne gravity Bouguer anomaly data (gravity data) were obtained in XYZ format; X and Y are distances in meters measured along east and north directions respectively, while Z is the Bouguer anomaly value measured in mgal.

3.1. Method of data analysis

Interpretation of airborne magnetic and gravity survey data is aimed at mapping the surface and subsurface regional structures (intrusive bodies, contacts, faults, basement rocks and mineralization). This is achieved by employing both quantitative and qualitative approaches.

Qualitative interpretation involves the description of the survey results and the explanation of the major features revealed by a survey in terms of the types of likely geological formations and structures that give rise to the evident anomalies [20]. The goal is to identify and delineate the anomalies and interpret them based on their constitution and geometry.

Gridding of potential field data is crucial in the analysis and processing workflow. This is because imaging, processing and interpretation require the data to be converted to an evenly spaced two-dimension (2-D) grid and this can be achieved via gridding. The minimum curvature method was employed to produce the grids, [21-22]. A grid size of 100m for the aeromagnetic data and 500m for the gravity data were applied. This was considered appropriate as it ensures that errors due to over or under-sampling based on the sampling distance of the two data are avoided. The gridding of the aeromagnetic and satellite gravity data produced the total magnetic intensity (TMI) and Bouguer anomaly maps, respectively.

The quantitative interpretation techniques adopted in this study are Source parameter imaging (SPI), Euler deconvolution and forward and inverse modelling for both the aeromagnetic and satellite gravity data. The first stage of quantitative aeromagnetic and satellite gravity data interpretation involved the application of mathematical filters. The main aim of data filtering is to enhance the anomalies or wavelength of interest, in order to gain preliminary information on source of magnetic and gravity anomalies. The different filtering methods employed include polynomial fitting, first vertical derivative (FVD), second vertical derivative (SVD) and horizontal derivative (HD).

Regional-residual separation was achieved using a second-order polynomial fit. The regional field was then removed from the total magnetic intensity map to obtain the residual anomalies. The residual intensity field is used to bring into focus, local features which tend to be obscured by the broad features of the regional field, in addition to residual anomalies are useful for structural mapping or qualitative interpretation based on visual inspection of the data [23]. This is done by applying the Butterworth filter in Oasis Montaj software. A derivative helps to sharpen the edge of the anomaly and enhance shallow features [20]. First vertical, second vertical and horizontal derivatives were applied to the data. The first vertical derivative is an enhancement technique that sharpens up anomalies over bodies and tends to reduce anomaly complexity, thereby allowing clear imaging of the causative structures. The second vertical derivative further sharpens the edges of causative bodies and amplifies fault geometry and trend, while horizontal derivative brings a directional perspective to the filter, further enhancing edges. This enhancement is designed to enhance faults and contact features. Maxima in the mapped enhancement indicates source edges [20].

In computing the SPI depth of the magnetic and gravity data, Oasis Montaj software was employed. Using the first vertical derivatives and horizontal gradient, the SPI function is a quick, easy and powerful method for calculating the depth of potential field sources. SPI has the advantage of producing a complete set of coherent solution points. Thurston and Smith [24] defined source parameter imaging as a profile or grid-based method used for estimating potential field source depths, and for some source geometries; the dip, susceptibility and density contrast. This method utilizes the relationship between source depth and the local wavenumber (k) of the observed field, which can be calculated for any point within a grid of data through horizontal and vertical gradients. At peaks in the local wavenumber grid, the source depth is equal to $\frac{n}{k}$, where n depends on the assumed source geometry (analogous to the structural index in Euler deconvolution); for example, n=1 for a horizontal contact, n=2 for a dyke. Peaks in the wavenumber grid are identified using a peak tracking algorithm [25] and valid depth estimates isolated. SPI method [24] used in this work estimates the depth from the local wavenumber of the analytical signal. The analytical signal A_1 (x, z) is defined by Nabighian [26] as:

$$A_1(x, z) = \frac{\partial M}{\partial x}(x, z) - j\frac{\partial M}{\partial z}(x, z) \quad (1)$$

where M (x, z) is the magnitude of the anomalous potential field; j is the imaginary number; x and z are Cartesian coordinates for the vertical and horizontal directions, respectively.

The result from work done by Nabighian [26] shows that the vertical and horizontal derivatives which comprise of the real and imaginary parts of the 2D analytical signal are related by:

$$\frac{\partial M}{\partial x}(x, z) \Leftrightarrow -\frac{\partial M}{\partial z}(x, z) \quad (2)$$

where <=> denotes a Hilbert transformation pair.

Thurston and Smith [24] gave the definition of the local wavenumber K, to be:

$$K_1 = \frac{\partial}{\partial x} tan^{-1}\left[\frac{\frac{\partial M}{\partial z}}{\frac{\partial M}{\partial x}}\right] \quad (3)$$

In computing the Euler depth for both aeromagnetic and satellite gravity data, Oasis Montaj software was employed. The Euler depths were estimated using vertical derivatives in three dimensions (x, y, and z). Vertical derivatives enhance shallow magnetic and gravity bodies. Hence, depths of shallow magnetic anomalies for different structural index were generated by applying Euler deconvolution method. The filter was applied for structural index 0, 1, 2, and 3 but as the goal was to find depth related to geological information, the structural index of 0 was employed.

Euler deconvolution method is an automatic technique used for location of the source of potential field based on both their amplitude and gradients. The Euler method satisfies the Euler's homogeneity equation given by [27]:

$$(x - x_o)\frac{\partial M}{\partial X} + (y - y_o)\frac{\partial M}{\partial y} + (z - z_o)\frac{\partial M}{\partial z} = -NM \quad (4)$$

where $\frac{\partial M}{\partial X}$, $\frac{\partial M}{\partial y}$ and $\frac{\partial M}{\partial z}$ represent first-order derivative of the potential field along x, y and z directions, respectively. N is the structural index which is related to the geometry of the magnetic and gravity source. Thompson [27] assigned N= 3 for sphere, N= 2 for pipe, N = 1 for thin dyke and N = 0 for horizontal contact body. Putting into consideration the base level of the regional potential field (D), equation (4) becomes:

$$x_o\frac{\partial M}{\partial X} + y_o\frac{\partial M}{\partial y} + z_o\frac{\partial M}{\partial z} + ND = x\frac{\partial M}{\partial X} + y\frac{\partial M}{\partial y} + z\frac{\partial M}{\partial z} + NM \quad (5)$$

The structural index (N) assigned to equations (4) and (5) helps in obtaining a system of linear equations and used in estimating the location and depth of the magnetic and gravity bodies.

Forward and inverse modelling techniques involve making numerical estimates of the depth and dimensions of the sources of anomalies and this often takes the form of modelling of sources which could, in theory, replicate the anomalies recorded in the survey [28]. The forward modelling being a trial and error method, the shape, position and physical properties of the model is adjusted in order to obtain a good correlation between the calculated field and the observed field data. The inverse modelling automatically adjusts itself to obtain the best fit

between the calculated and the observed field. The software used for the modelling and inversion of the anomalies is Oasis Montaj, which contains potent software. Potent is a program for modelling the magnetic and gravitational effects of the subsurface. Interpretation of potential field data using potent starts with observation of the image of the observed data [29].

4. Results and discussion

From qualitative interpretation, the total magnetic intensity (TMI) map (Figure 4a) produced using the minimum curvature method of the Oasis Montaj software shows the general magnetic anomaly of the basement rocks and the inherent variation in the basin under study. The TMI values range from -137.7 to 160.6 nT. The TMI map of Gubio area revealed that the area is magnetically heterogeneous. Areas of very strong magnetic values (139.0 to 160.6 nT) are caused probably by near-surface igneous or metamorphic rocks of high magnetic susceptibility values. The areas between -137.7 to -34.9 nT are most likely due to thick sedimentary deposits and the presence of other non-magnetic sources like sandstones.

The bouguer anomaly of the study area varies from -46.9 to 9.6 mgal (Figure 4b). The colour legend bar identifies regions of gravity high (red and pinks) which corresponds to a region with high-density contrast beneath the surface; intermediate values (green and yellow) and gravity lows (blue colour) that correspond to regions of low-density contrast.

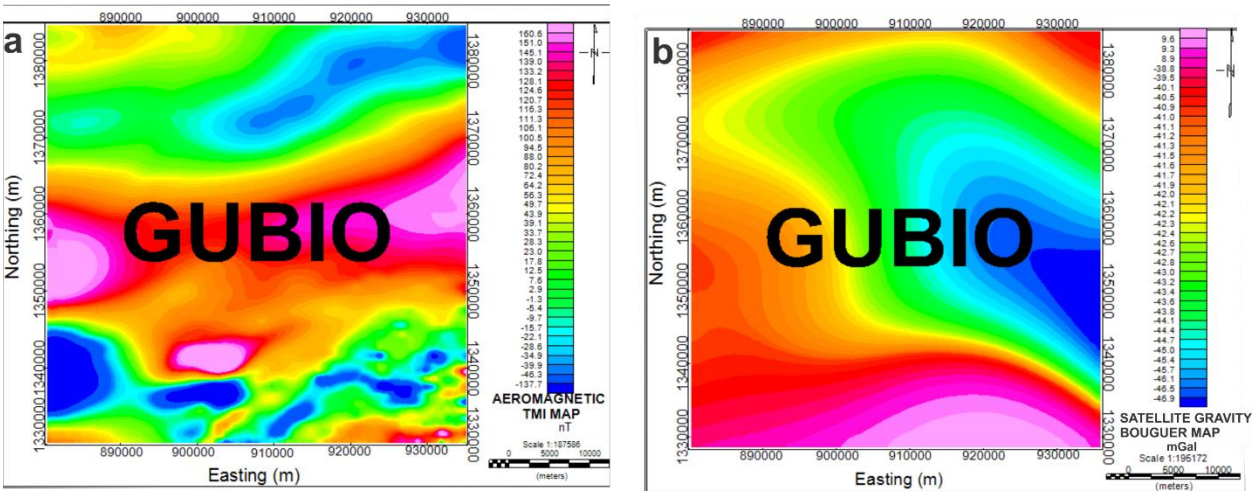

Fig. 4. (a) TMI map and (b) Bouguer anomaly map of the study area

The first vertical derivative computed on the residual data of both aeromagnetic and satellite gravity enhanced the shallow sources by suppressing the effect of the deeper ones. This helped to reveal near-surface intrusions (Figure 5a and 5b). The second vertical derivative sharpens the effect of the first vertical derivatives and helps to determine the edge of the anomalous body (Figure 5c and 5d). The horizontal derivative shows a more exact location for linear features which may include faults and folds (Figure 5e and 5f).

The computed SPI depths for aeromagnetic and satellite gravity are shown in Figures 6a and 6b respectively, the negative depth values shown on the SPI legend depicts the depths of buried magnetic and gravity bodies, which may be deep-seated basement rocks or near-surface intrusive. The pink colour generally indicates areas occupied by shallow magnetic/gravity bodies, while the blue colour depicts areas of deep-lying magnetic/gravity bodies. The SPI depth result ranges from -381.7 m to -4610.5 m for aeromagnetic data and from -1009.3 to -4511.9 m for satellite gravity data.

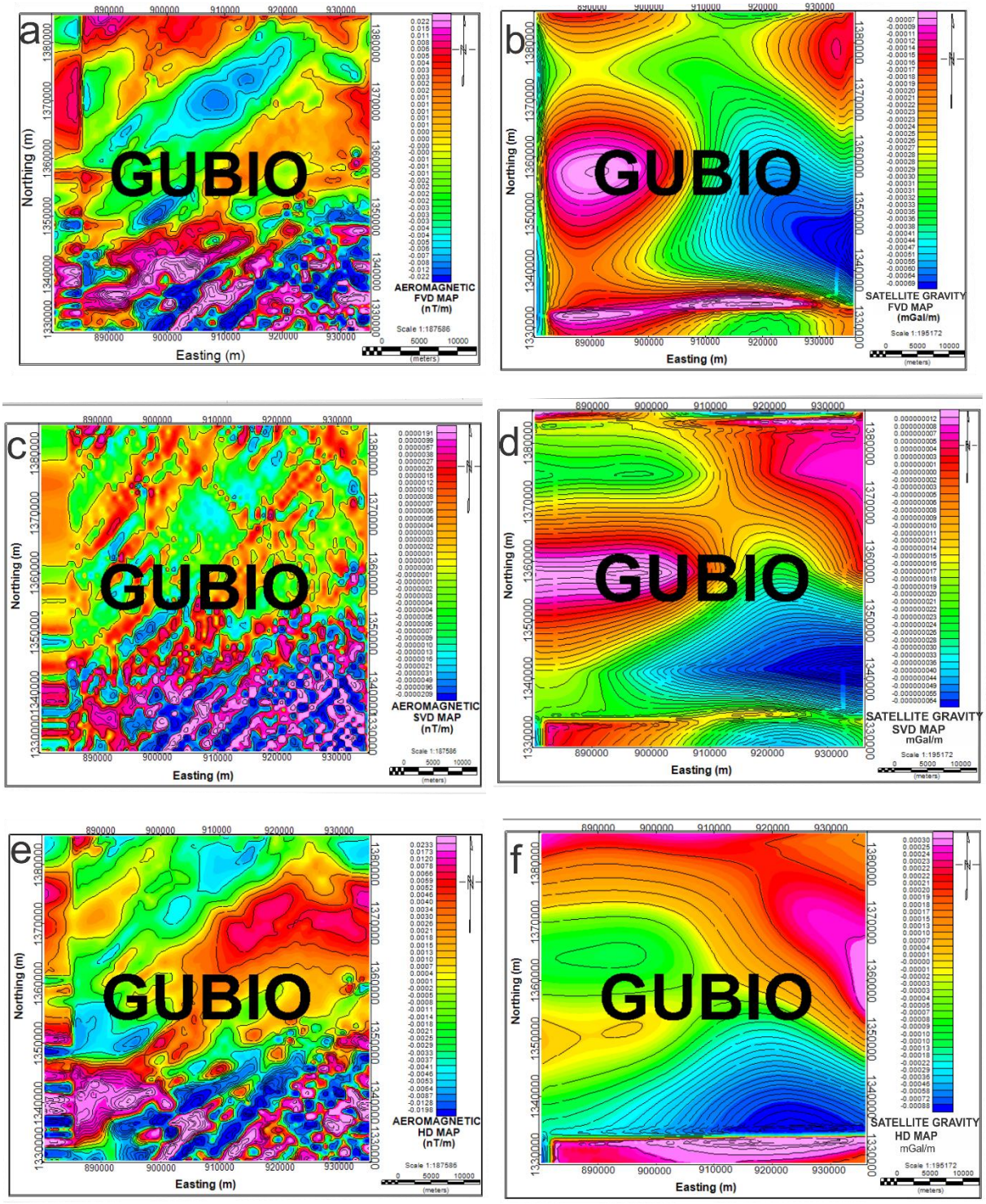

Fig. 5. Magnetic and gravity filtering (a) first vertical derivative map (magnetic), (b) Satellite gravity first vertical derivative map, (c) Aeromagnetic second vertical derivative map, (d) Satellite gravity second vertical derivative map, (e) Aeromagnetic horizontal derivative map, (f) Satellite gravity horizontal derivative map.

For the Euler deconvolution method, two Euler deconvolution maps were generated, as shown in Figure 7 (a, b) for magnetic and gravity data. The Euler depth result ranges from 1260.5 m (outcropping magnetic bodies) to -3968.5 m (deep-lying magnetic bodies) for the

aeromagnetic and 1696.8 m (outcropping Bouguer anomalous bodies) to -4371.2 m (deep-lying Bouguer anomalous bodies) for the satellite gravity.

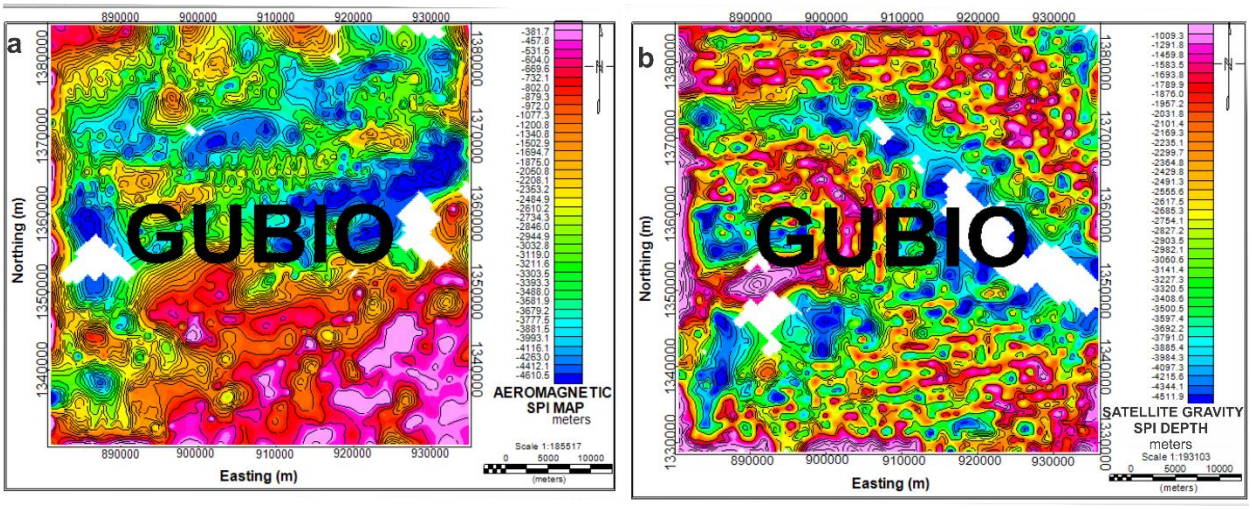

Fig. 6. SPI map; (a) for aeromagnetic data, (b) for aeromagnetic gravity data

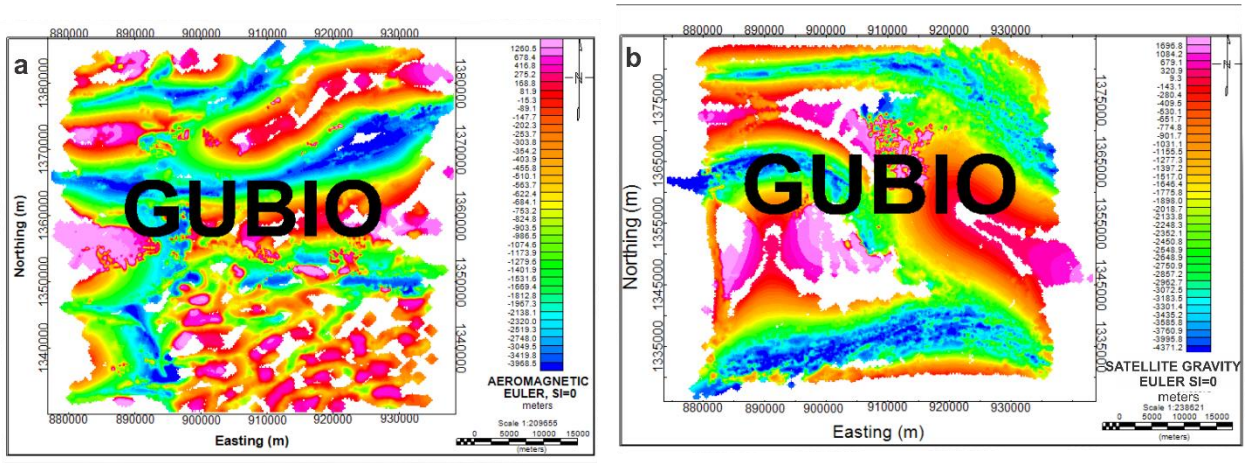

Fig. 7. Euler 3D depth map for SI=0; (a) Magnetic data, (b) gravity data

Figure 8a shows the position six profiles taken on the residual magnetic map. Each profile produced a degree of strike, dip and plunge where the observed values matched well with the calculated values. Using Potent Q 3D plugin of the Oasis Montaj software, the field of the models were calculated. The result of the forward and inverse modelling of the aeromagnetic data is summarized on Table 1. The estimated depths from forward and inverse modelling of aeromagnetic data for profiles 1-6 are 709, 722, 2052, 1836, 4365 and 877 m, respectively, with corresponding susceptibility values of 0.0003, 0.017, 0.04, 0.025, 0.0002, and -0.0001 SI. For satellite gravity data interpretation, the first vertical derivative gravity grid was modelled and density of causative bodies obtained from modelling results for profiles 7 and 8 (Figure 8b) were 2.700 and 2.630 g/cm^3 with respective depths to the surface of 3460 and 1250 m. The result of the forward and inverse modelling for satellite gravity is summarized in Table 2.

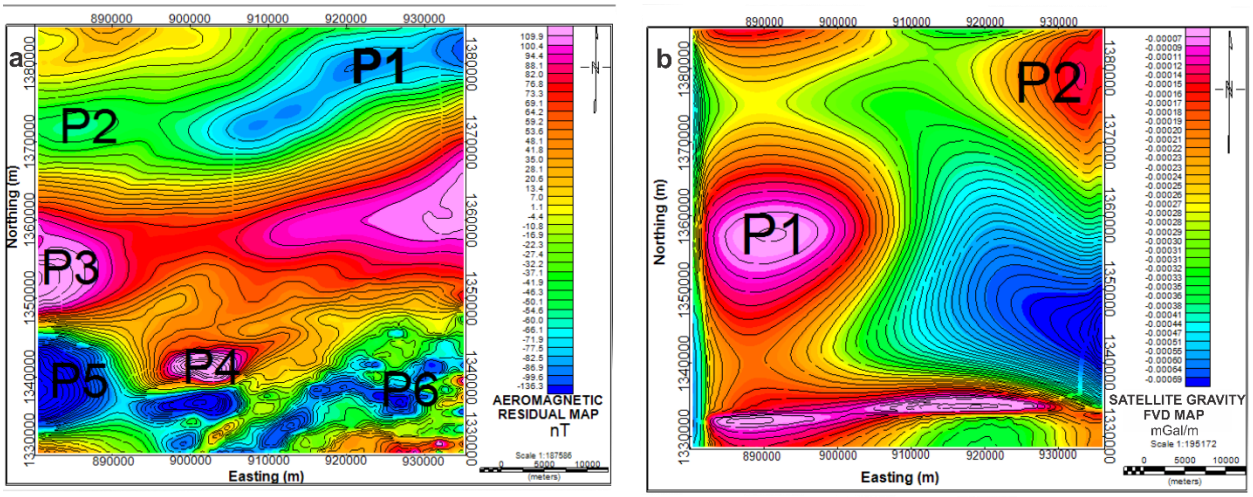

Fig. 8. (a) Aeromagnetic residual contour map of Gubio showing six profile locations and (b) Satellite gravity FVD contour map of Gubio showing two profile locations

Figure 9(a-h) shows correlation between the calculated field and the observed field data. The blue curves represent the observed field values, while the red curves represent the calculated field values for the six profiles from aeromagnetic data and two profiles from satellite gravity data.

Table 1. Summary of aeromagnetic forward and inverse modelling results

Model	Model shape	X(m)	Y(m)	Depth to anomalous body (m)	Plunge (deg)	Dip (deg)	Strike (deg)	K-value (SI)
P1	Rectangular Prism	921361	1380475	709	-24.5	75.8	-78.0	0.0003
P2	Ellipsoid	885478	1372407	722	0.6	-11.7	-97.0	0.017
P3	Ellipsoid	882871	1350161	2052	156.1	74.2	-127.4	0.04
P4	Rectangular Prism	901032	1340314	1836	5.1	-48.7	-57.9	0.025
P5	Rectangular Prism	882794	1337029	4365	-6.9	-105.6	-70.8	0.0002
P6	Ellipsoid	926548	1336244	877	-43.2	95.5	51.0	0.0001

Table 2. Summary of satellite gravity forward and inverse modelling results

Model	Model shape	X(m)	Y(m)	Depth to anomalous body (m)	Plunge (deg)	Dip (deg)	Strike (deg)	Density value (g/cm^3)
P1	Ellipsoid	888904	1357838	3460	15.8	33.6	-132.9	2.700
P2	Ellipsoid	932188	1379083	1250	2.6	3.6	-168.0	2.630

The average depth ranges (2052 – 3460) obtained from different methods in this work suggest a fairly thick sedimentary pile that favour hydrocarbon generation and accumulation.

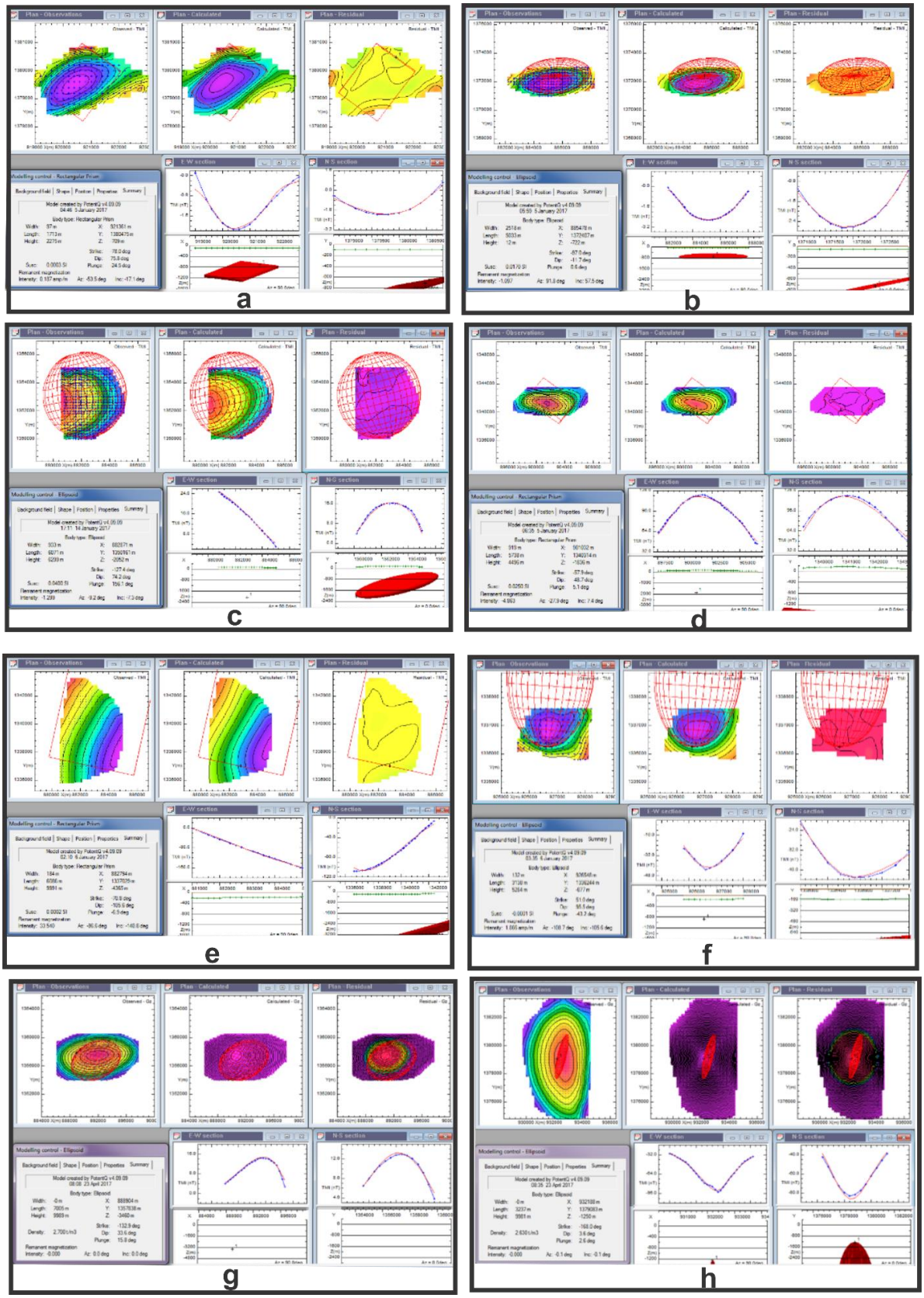

Fig. 9. Subset of (a) profile 1, (b) profile 2, (c) profile 3, (d) profile 4, (e) profile 5, (f) profile 6 (aero-magnetic data), (g) profile 7 and (h) profile 8 for satellite gravity data

5. Conclusion

The aeromagnetic and satellite gravity data of Gubio area, Chad Basin, Nigeria, were interpreted qualitatively and quantitatively. The total magnetic intensity and residual intensity field reveal a range of magnetic anomalies which reveal that the study area is magnetically heterogeneous. The bouguer gravity anomaly map identifies regions of gravity high, which corresponds to a region with high-density contrast and gravity lows which correspond to regions of low-density contrast. The horizontal derivative shows the occurrence of subsurface linear structures. These features can be investigated further using seismic data to determine their suitability as structural traps.

Acknowledgement

The authors wish to thank the Nigerian Geological Survey Agency (NGSA) for providing the aeromagnetic data and National Aeronautics and Space Administration (NASA) for providing the satellite gravity data.

References

[1] Genik GJ. Petroleum Geology of Cretaceous-Tertiary Rift Basins in Niger, Chad, and Central African Republic. The American Association of Petroleum Geologists Bulletin, 1993; 77(5):1405-1434.

[2] Hamza H, Hamidu I. Hydrocarbon resource potential of the Bornu Basin northeastern Nigeria. Global Journal of Geological Sciences, 2011; 10(1):71-84.

[3] Okonkwo CC, Onwuemesi AG, Anakwuba EK, Chinwuko AI, Ikumbur BE, Usman AO. Aeromagnetic Interpretation over Maiduguri and Environs of Southern Chad Basin, Nigeria. Journal of Earth Sciences and Geotechnical Engineering, 2012; 2(3): 77-93.

[4] Olugbemiro RO, Ligouis B, Abaa SI. The Cretaceous series in the Chad Basin, NE Nigeria: Source rock potential and thermal maturity. Journal of Petroleum Geology, 1997; 20(1):51-68.

[5] Olabode SO, Adekoya JA, Ola PS. Distribution of sedimentary Formations in the Bornu Basin Nigeria. Petroleum Exploration and Development, 2015; 42(5):674-682.

[6] Zarma AA, Tukur A. Stratigraphic status of the Bama Beach Ridge and the Chad Formation in the Bornu Sub-basin, Nigeria. Journal of Geology and Geophysics, 2015; 4(1):1-7.

[7] Avbovbo AA, Ayoola EO, Osahon GA. Depositional and structural styles in Chad Basin of Northeastern Nigeria. Bulletin American Association Petroleum Geologists, 1986; 70(121): 1787 – 1798.

[8] Nwankwo CN, Emujakpowe GO, Nwosu LI. Evaluation of the petroleum potentials and prospect of the Chad Basin Nigeria from heat flow and gravity data. Journal of Petroleum Exploration and Production Technology, 2012; 2:1-6.

[9] Ola PS, Adekoya JA, Olabode SO. Source rock evaluation of the southwest portion of the Bornu Basin, Nigeria: IOSR Journal of Applied Geology and Geophysics, 2018; 6(3):27-31.

[10] Nwankwo CN, Ekine AS. Geothermal gradients in the Chad Basin, Nigeria from bottom hole temperature logs. International Journal of Physical Sciences, 2009; 4(12):777-783.

[11] Anakwuba EK, Chinwuko AI. One dimensional spectral analysis and curie depth isotherm of Eastern Chad Basin, Nigeria. Journal of Natural Science Research, 2015; 5(19):14-23.

[12] Goni IB, Nur A, Mbusube AM, Yusuf SN, Sheriff BM. Estimating the sedimentary thickness of the Bornu Basin using spectral analyses of high-resolution aeromagnetic data. Journal of Mining and Geology, 2016; 52(1): 83-92.

[13] Arogundade AB, Hammed OS, Awoyemi MO, Falade SC, Ajana OD, Olayode FA, Adebayo AS, Olabode AO. Analysis of aeromagnetic anomalies of parts of Chad Basin, Nigeria, using high-resolution aeromagnetic data. Modeling Earth Systems and Environment, 2020; 6(3):1545-1556.

[14] Burke KC. The Chad Basin: an active intra-continental basin. Tectonophysics, 1976; 36:197-206.

[15] Binks RM, Fairhead JD. A plate tectonic setting for Mesozoic rifts of West and Central Africa. In P.A. Ziegler (Editor), Geodynamics of rifting, volume II case history studies on rifts: North and South America and Africa. Tectonophysics, 1992; 213:141-151.

[16] Genik GJ. Regional framework, structural and petroleum aspects of rift basins in Niger, Chad and the Central African Republic (C.A.R) In P.A. Ziegler (Editor), Geodynamics of rifting, volume II case history studies on rifts: North and South America and Africa. Tectonophysics, 1992; 213:169-185.

[17] Nwajide SC. Geology of Nigeria's Sedimentary Basins. CSS Bookshops Ltd. Lagos, 2013; 565pp.

[18] Kogbe CA. Paleogeograhic History of Nigeria from Albian times. In Geology of Nigeria (Ed) by Kogbe C.A. Elizabethan Publishers, Lagos, 1976; 237-252.
[19] Oha IA, Onuoha KM, Nwegbu AN, Abba AU. Interpretation of high-resolution aeromagnetic data over Southern Benue Trough, Southeastern Nigeria. Journal of Earth System Science, 2016; 125:369-385.
[20] Revees C. Aeromagnetic Surveys; Principles, Practice and Interpretation. GEOSOFT, 2005; 155pp.
[21] Briggs IC. Machine contouring using minimum curvature. Geophysics, 1974; 39:39-48.
[22] Webring M. MINC: a gridding program based on minimum curvature. U.S. Geological Survey, 1981; 43: 81-1224.
[23] Alagbe OA, Sunmonu, LA. Interpretation of Aeromagnetic Data from Upper Benue Basin, Nigeria Using Automated Techniques. IOSR Journal of Applied Geology and Geophysics, 2014; 2:22-40.
[24] Thurston JB, Smith RS. Automatic conversion of magnetic data to depth, dip, and susceptibility contrast using the SPI™ method. Geophysics, 1997; 62(3):807-813.
[25] Blakely RJ, Simpson RW. Approximating edges of source bodies from magnetic or gravity anomalies. Geophysics, 1986; 51:1494-1498.
[26] Nabighian MN. The analytic signal of two-dimensional magnetic bodies with polygonal cross-section: Its properties and use for automated anomaly interpretation. Geophysics, 1992; 37(3): 507-517.
[27] Thompson DT. A new technique for making computer-assisted depth estimates from magnetic data. Geophysics, 1982; 47(1): 31-37.
[28] Bonde DS, Udensi E E, Momoh M. Modelling of Magnetic Anomaly zones in Sokoto Basin, Nigeria. Journal of Applied Geology and Geophysics, 2014; 2(1): 19-25.
[29] Obiora DN Yakubu JN, Okeke FN, Chukwudebelu, JU, Oha AI. Interpretation of aeromagnetic data of Idah area in North Central Nigeria using combined methods. Journal of the geological society of India, 2015; 88:98-106.

To whom correspondence should be addressed: Dr. Ifeanyi. A. Oha, Department of Geology, University of Nigeria, Nsukka, Enugu State, Nigeria, E-mail: *ifeanyi.oha@unn.edu.ng*